Distorted Trigonal Prismatic Coordination in Tris(9,10-phenanthrenequinone)molybdenum

Cortlandt G. Pierpont* and Robert M. Buchanan

Contribution from the Department of Chemistry, West Virginia University, Morgantown, West Virginia 26506. *Received November 21, 1974*

Abstract: The complex $Mo(PQ)_3$ has been synthesized by reaction of $Mo(CO)_6$ with 9,10-phenanthrenequinone and examined structurally. Crystals of $Mo(PQ)_3$ are triclinic, space group $P\bar{1}$ with a = 12.251 (3) Å, b = 10.825 (3) Å, c = 16.632 (4) Å, α = 112.19 (5)°, β = 125.26 (5)°, γ = 96.44 (5)°, ρ(obsd) = 1.58 (1) g/cm^3, and ρ(calcd) = 1.573 g/cm^3 for two molecules per unit cell. The structure was solved by conventional Patterson, Fourier, and least-squares procedures using X-ray data complete to 2θ = 50° (Mo Kα radiation). Refinement of the structure converged with final discrepancy indices of R = 0.047 and R_w = 0.048 for 2182 independent, observed reflections. The PQ ligands are chelated to the Mo with a trigonal prismatic geometry for the MoO_6 polyhedron. One ligand of the $Mo(PQ)_3$ molecule is bent away from its MoO_2 chelate plane forming a dihedral angle of 119.7 (6)° between this plane and the carbon atoms of the ligand. This distortion appears to result from formation of a strong, intermolecular charge-transfer dimer between centrosymmetrically related complex molecules. Separation between ligand planes of adjacent molecules is approximately 3.2–3.3 Å. Carbon–oxygen distances of the bent ligand (1.31 (1) Å) suggest greater benzoquinone character than values of the planar chelated ligands (1.35 (1) Å).

Transition metal complexes of *o*-benzoquinones have been known for many years but only recently have significant steps been taken toward understanding the true nature of metal–quinone bonding. Renewed interest in quinone complexes stems from the use of *o*-benzoquinones as agents in oxidative-addition reactions to basic metals,[1] their relevance to metal catalyzed biological redox reactions of quinones[2] and quinoid[3] molecules, and the analogy of these ligands to the interesting 1,2-dithiolene systems.[4] While the number the quinone complexes is large there are relatively few examples of simple, homologated complexes with transition metals. Neutral complexes of Ni, Co, and Fe with tetrachloro-1,2-benzoquinone[5] and 9,10-phenanthrenequinone[6] have been synthesized by direct reaction of the benzoquinone with an appropriate metal carbonyl. Much earlier tris(1,2-benzoquinone)tungsten was formed by reaction of catechol with WCl_6.[7] Little more than chemical composition is known about these compounds, and they clearly deserve further study.

We have recently examined the addition of tetrachloro-1,2-benzoquinone to carbonyls of the metals Cr, Mo, and W yielding the neutral tris complexes, $M(O_2C_6Cl_4)_3$.[8] In contrast to the trigonal prismatic coordination geometries of the 1,2-dithiolene analogs, the quinone complexes have octahedral structures with dimeric geometries for the Mo and W compounds.[9] Some of the unusual structural features observed for the Mo complex $[Mo(O_2C_6Cl_4)_3]_2$ include the discovery of both bridging and chelating quinone ligands, short oxygen–oxygen contacts along meridional edges of the octahedron and the formation of intermolecular linkages through bridges formed by benzene solvate charge-transfer interactions. In an effort to extend this work to other *o*-benzoquinones the reaction between $Mo(CO)_6$ and 9,10-phenanthrenequinone (PQ) has been carried out. The results of this synthesis have led to the formation of two new compounds, an oxomolybdenum species, $Mo_2O_5(PQ)_2$,[10] and tris(9,10-phenanthrenequinone)molybdenum, closely related to $[Mo(O_2C_6Cl_4)_3]_2$. To examine this relationship and further clarify the coordination properties of *o*-benzoquinones the molecular structure of $Mo(PQ)_3$ has been determined crystallographically.

Experimental Section

Synthesis of $Mo(O_2C_{14}H_8)_3$. A mixture containing 2.0 g of 1,10-phenanthrenequinone and 0.5 g of $Mo(CO)_6$ was refluxed in methylene chloride for 6 hr under nitrogen. If carried out in the dark no visible reaction occurs. However, in the presence of the fluorescent lights of the laboratory, the yellow solution becomes dark green over the period of a few hours. Upon concentration of the solution, a crude green precipitate formed which has subsequently been identified as a mixture of the green complex $Mo_2O_5(PQ)_2$ and excess quinone. Soxhlet extraction of the green mixture with benzene resulted in a blue solution from which appeared crystals of the violet complex $Mo(PQ)_3$. Crystals of $Mo(PQ)_3$ form as pleochioic plates appearing red when viewed down the large face but when ground to powder appear violet. The choice of CH_2Cl_2 as the solvent for the initial reaction appears critical since crude products formed from other solvent media fail to yield $Mo(PQ)_3$.

Collection and Reduction of the X-Ray Data. Precession and Weissenberg photographs on crystals of $Mo(PQ)_3$ indicated triclinic symmetry. A crystal of dimensions 0.10 × 0.24 × 0.32 mm was aligned on a Picker four-circle diffractometer. Lattice constants determined at ambient room temperature from least-squares refinement of the angular settings of 21 strong, independent reflections located using Mo Kα radiation are a = 12.251 (3) Å, b = 10.825 (3) Å, c = 16.632 (3) Å, α = 112.19 (5)°, β = 125.26 (5)°, and γ = 96.44 (5)°. An experimental density of 1.58 (1) g/cm^3 agrees with a calculated value of 1.573 g/cm^3 for two $Mo(O_2C_{14}H_8)_3$ molecules per unit cell. Thus space group $P\bar{1}$ was chosen for the refinement. The mosaic spread of the crystal determined using the narrow-source open-counter ω-scan technique was acceptable at 0.06°.[11] An independent set of intensity data was collected by the θ–2θ scan technique using the Zr filtered Mo Kα peak with allowances made for the Kα_1–Kα_2 separation at higher 2θ values. The data set was collected within the angular range $4.5 \geq 2\theta \geq 50°$. Attenuators were inserted automatically if the count rate of the diffracted beam exceeded 9000 counts/sec during the scan. During data collection the intensities of five standard reflections in different regions of reciprocal space were monitored after every 100 reflections measured. None of these standards deviated from its mean value by more than 5% during the time required to collect data. Data were processed in the usual way with values of I and $\sigma(I)$ corrected for Lorentz and polarization effects. No correction for absorption was made since the linear absorption coefficient is small (μ = 4.9 cm^{-1}) and rotation of the crystal at X = 90.00° showed only a 5% variation in intensity of a reflection coincident with the ϕ axis of the instrument. The intensities of a total of 5224 reflections were measured, of which 2182 were observed to be greater than 2σ and have been included in the refinement. While this number is somewhat low the crystal chosen for data collection diffracted most strongly of the single-crystals obtained.

Solution and Refinement of the Structure. The position of the Mo atom was determined from a three-dimensional Patterson map. Phases derived from the Mo were used to locate all other non-hydrogen atoms of the structure. Isotropic refinement of all atoms gave discrepancy indices $R = \Sigma||F_o| - |F_d||/\Sigma|F_o|$ and $R_w = (\Sigma w|F_o| - |F_d|)^2/\Sigma wF_o^2)^{1/2}$ of 0.073 and 0.074, respectively. Fur-

Table I. Final Atomic Positional and Thermal Parameters for $Mo(O_2C_{14}H_8)_3$

Atom	x^a	y	z	$\beta_{11}{}^b$	β_{22}	β_{33}	β_{12}	β_{13}	β_{23}
Mo	−0.0161 (1)	0.1989 (1)	0.1337 (1)	0.0105 (1)	0.0112 (1)	0.0065 (1)	0.0042 (1)	0.0061 (1)	0.0046 (1)
O(1)	0.0765 (6)	0.0637 (6)	0.1574 (4)	0.0109 (10)	0.0132 (10)	0.0075 (7)	0.0044 (8)	0.0072 (7)	0.0051 (7)
O(2)	−0.1986 (6)	0.0162 (6)	0.0371 (4)	0.0125 (10)	0.0122 (10)	0.0065 (6)	0.0054 (8)	0.0064 (7)	0.0049 (7)
O(3)	0.1148 (6)	0.2560 (6)	0.1101 (4)	0.0107 (10)	0.0108 (10)	0.0063 (6)	0.0047 (8)	0.0053 (7)	0.0047 (6)
O(4)	−0.1436 (6)	0.2108 (6)	−0.0023 (10)	0.0123 (10)	0.0137 (10)	0.0087 (6)	0.0049 (8)	0.0086 (7)	0.0059 (7)
O(5)	0.1560 (6)	0.3471 (6)	0.2997 (5)	0.0125 (10)	0.0136 (10)	0.0092 (7)	0.0072 (9)	0.0085 (8)	0.0068 (7)
O(6)	−0.1035 (6)	0.3063 (6)	0.1867 (5)	0.0084 (9)	0.0113 (10)	0.0049 (6)	0.0026 (8)	0.0037 (6)	0.0029 (6)

Atom	x^a	y	z	$\beta_{11}{}^b$	Atom	x^a	y	z	$\beta_{11}{}^b$
C(1)	0.0129 (9)	0.0209 (9)	0.1902 (7)	2.7 (2)[c]	C(22)	0.3821 (9)	0.4312 (9)	0.0529 (7)	3.9 (3)[c]
C(2)	−0.1395 (9)	−0.0067 (9)	0.1225 (7)	3.2 (3)	C(23)	0.3129 (9)	0.4668 (9)	−0.0326 (7)	3.9 (3)
C(3)	−0.2211 (9)	−0.0587 (9)	0.1497 (7)	3.6 (3)	C(24)	0.1670 (9)	0.4411 (9)	−0.0978 (7)	3.6 (3)
C(4)	−0.1507 (10)	−0.0882 (9)	0.2400 (7)	3.9 (3)	C(25)	−0.3089 (10)	0.2594 (9)	−0.1921 (7)	3.8 (3)
C(5)	0.0037 (9)	−0.0569 (9)	0.3092 (7)	3.6 (3)	C(26)	−0.3773 (9)	0.2938 (9)	−0.2764 (7)	4.1 (3)
C(6)	0.0859 (9)	−0.0011 (9)	0.2860 (7)	3.4 (3)	C(27)	−0.2968 (10)	0.3565 (9)	−0.2973 (7)	4.1 (3)
C(7)	0.2392 (10)	0.0351 (9)	0.3554 (8)	4.2 (3)	C(28)	−0.1514 (9)	0.3799 (9)	−0.2381 (7)	3.8 (3)
C(8)	0.3075 (11)	0.0094 (10)	0.4440 (8)	5.3 (3)	C(29)	0.1342 (9)	0.4374 (9)	0.3651 (7)	3.0 (2)
C(9)	0.2249 (11)	−0.0529 (10)	0.4690 (8)	5.6 (3)	C(30)	−0.0089 (9)	0.4145 (9)	0.3029 (8)	3.2 (2)
C(10)	0.0751 (10)	−0.0858 (10)	0.3988 (8)	5.1 (3)	C(31)	−0.0574 (9)	0.5086 (9)	0.3550 (7)	3.2 (3)
C(11)	−0.3742 (10)	−0.0861 (9)	0.0806 (8)	4.6 (3)	C(32)	0.0581 (9)	0.6267 (9)	0.4758 (7)	3.4 (3)
C(12)	−0.4562 (11)	−0.1459 (10)	0.1022 (8)	5.3 (3)	C(33)	0.2095 (10)	0.6511 (9)	0.5397 (8)	3.8 (3)
C(13)	−0.3879 (11)	−0.1735 (10)	0.1889 (8)	5.5 (3)	C(34)	0.2496 (9)	0.5568 (9)	0.4870 (7)	3.3 (3)
C(14)	−0.2403 (11)	−0.1435 (10)	0.2592 (8)	5.0 (3)	C(35)	0.3987 (10)	0.5762 (10)	0.5499 (8)	4.6 (3)
C(15)	0.0612 (9)	0.2841 (8)	0.0251 (7)	2.6 (2)	C(36)	0.5110 (11)	0.7004 (11)	0.6665 (9)	5.7 (3)
C(16)	−0.0824 (9)	0.2586 (9)	−0.0370 (7)	2.7 (2)	C(37)	0.4706 (12)	0.7932 (11)	0.7178 (8)	6.0 (4)
C(17)	−0.1575 (9)	0.2871 (8)	−0.1267 (7)	3.1 (2)	C(38)	0.3265 (11)	0.7711 (10)	0.6589 (8)	5.1 (3)
C(18)	−0.0758 (9)	0.3495 (8)	−0.1486 (7)	2.8 (2)	C(39)	−0.2077 (9)	0.4792 (9)	0.2883 (7)	3.9 (3)
C(19)	0.0784 (8)	0.3777 (8)	−0.0815 (7)	2.7 (2)	C(40)	−0.2465 (11)	0.5693 (10)	0.3425 (8)	4.8 (3)
C(20)	0.1493 (9)	0.3441 (9)	0.0062 (7)	3.1 (3)	C(41)	−0.1364 (11)	0.6877 (10)	0.4609 (8)	4.3 (3)
C(21)	0.2998 (9)	0.3699 (8)	0.0716 (7)	3.2 (3)	C(42)	0.0094 (10)	0.7143 (9)	0.5255 (7)	4.3 (3)

[a] Estimated standard deviations of the least significant figures are given in parentheses. [b] Anisotropic thermal parameters are in the form $\exp[-(h^2\beta_{11} + k^2\beta_{22} + l^2\beta_{33} + 2hk\beta_{12} + 2hl\beta_{13} + 2kl\beta_{23})]$. [c] Atoms refined with isotropic thermal parameters.

ther refinement with anisotropic thermal parameters for the Mo and O atoms gave discrepancy indices of $R = 0.055$ and $R_w = 0.061$. The positions of all hydrogen atoms were determined from a Fourier map and included in the refinement giving final discrepancy indices of $R = 0.047$ and $R_w = 0.048$. During all cycles of refinement the function minimized was $\Sigma w(|F_o| - |F_c|)^2$ and the weights, w, were taken as $4F_o{}^2/\sigma^2(F_o{}^2)$. The standard deviations $\sigma(F^2)$ were estimated by procedures described previously.[12] In all calculations the atomic scattering factors for the non-hydrogen atoms were those of Cromer and Waber[13] with hydrogen scattering factors taken from the report of Stewart et al.[14] The effects of anomalous dispersion were included in the calculated structure factors with values of $\Delta f'$ and $\Delta f''$ for the Mo atom taken from the report of Cromer and Liberman.[15] At the completion of the refinement the standard deviation of an observation of unit weight was 1.02. The final positional and thermal parameters of all nonhydrogen atoms are presented in Table I. Root-mean-square vibrational amplitudes of atoms refined anisotropically appear in Table II. Positional and thermal parameters of the hydrogen atoms appear in Table III. A table of the final F_o and F_c values is available.[16]

Table II. Root-Mean-Square Amplitudes of Vibration of Atoms Refined Anisotropically

Atom	Min (Å)	Intermed (Å)	Max (Å)
Mo	0.181 (1)	0.209 (1)	0.224 (1)
O(1)	0.166 (11)	0.224 (10)	0.247 (9)
O(2)	0.194 (10)	0.225 (14)	0.227 (11)
O(3)	0.199 (10)	0.211 (10)	0.216 (9)
O(4)	0.156 (11)	0.238 (8)	0.255 (9)
O(5)	0.186 (10)	0.223 (9)	0.249 (9)
O(6)	0.176 (10)	0.205 (10)	0.240 (9)

Table III. Refined Positional and Thermal Parameters of Hydrogen Atoms

Atom	x	y	z	B, Å^2
HC(7)	0.305 (7)	0.080 (7)	0.339 (6)	6.(2)
HC(8)	0.428 (7)	0.041 (7)	0.502 (6)	7.(2)
HC(9)	0.263 (7)	−0.033 (7)	0.462 (5)	5.(2)
HC(10)	0.013 (7)	−0.127 (7)	0.425 (6)	6.(2)
HC(11)	−0.427 (7)	−0.069 (7)	0.008 (6)	6.(2)
HC(12)	−0.567 (7)	−0.173 (7)	0.040 (5)	8.(2)
HC(13)	−0.441 (7)	−0.205 (7)	0.223 (6)	4.(2)
HC(14)	−0.176 (7)	−0.162 (7)	0.322 (6)	6.(2)
HC(21)	0.353 (7)	0.336 (7)	0.132 (6)	5.(2)
HC(22)	0.496 (7)	0.455 (7)	0.103 (6)	9.(2)
HC(23)	0.381 (7)	0.514 (7)	−0.044 (5)	5.(2)
HC(24)	0.123 (7)	0.474 (7)	−0.154 (6)	6.(2)
HC(25)	−0.371 (7)	0.193 (7)	−0.183 (5)	10.(3)
HC(26)	−0.497 (7)	0.282 (7)	−0.323 (6)	8.(2)
HC(27)	−0.351 (7)	0.383 (7)	−0.366 (6)	7.(2)
HC(28)	−0.074 (7)	0.434 (7)	−0.241 (6)	8.(2)
HC(35)	0.414 (7)	0.480 (7)	0.509 (6)	6.(2)
HC(36)	0.583 (7)	0.667 (7)	0.686 (5)	10.(3)
HC(37)	0.568 (7)	0.886 (7)	0.822 (6)	9.(3)
HC(38)	0.302 (7)	0.850 (7)	0.700 (5)	9.(3)
HC(39)	−0.303 (7)	0.376 (7)	0.196 (5)	6.(2)
HC(40)	−0.357 (7)	0.553 (7)	0.300 (5)	5.(2)
HC(41)	−0.184 (7)	0.731 (7)	0.494 (5)	7.(2)
HC(42)	0.100 (7)	0.808 (7)	0.616 (5)	8.(2)

Description of the Structure

In contrast to the dimeric, octahedral geometry of the related tetrachloro-1,2-benzoquinone complex of molybdenum, $[Mo(O_2C_6Cl_4)_3]_2$, the geometry of the MoO_6 polyhedron in $Mo(PQ)_3$ is trigonal prismatic. The stereochemical properties of $Mo(PQ)_3$ appear more closely related to the trigonal prismatic 1,2-dithiolene[17-20] and 1,2-diselenolene[21] complexes of Mo. In the present case the ideal D_{3h} symmetry of the sulfur and selenium donor complexes is disrupted by one chelated ligand bent out of its MoO_2 plane. This distortion from the simple planar chelated geometry of the other two ligands results from a relatively strong intermolecular charge-transfer interaction between bent and planar ligands of adjacent complex molecules related by a crystallographic center of inversion. A view of the inner coordination geometry of the complex is shown in Fig-

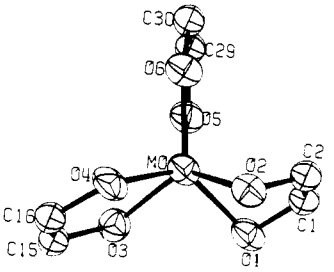

Figure 1. View of the inner coordination geometry of $Mo(PQ)_3$. Oxygens (1) and (2) are associated with the bent quinone ligand.

ure 1 with a stereoview of the full molecule in Figure 2. Figure 3 contains a view of both molecules of the unit cell. Pertinent bond distances and angles are given in Table IV with dihedral angles and least-squares planes in Table V.

Coordination of *o*-Quinone Ligands. The quinones seem to be a remarkably diverse series of ligands. While *p*-benzoquinones are known to coordinate as diene ligands, bonding to metals through localized olefin bonds of the ring,[22] the *o*-benzoquinones bond exclusively through their oxygens. Addition of tetrachloro-1,2-benzoquinone to $Mo(CO)_6$ yields $[Mo(O_2C_6Cl_4)_3]_2$. Structural characterization of this complex has shown that each metal possesses two chelated ligands with two additional ligands bridging the metals (I).[9]

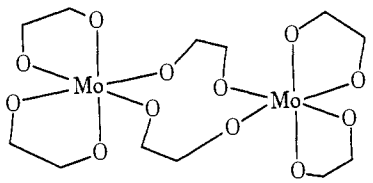

I

Longer C–O distances of the bridging ligands (1.37 (1) Å) reflect greater hydroquinone character than the planar chelating ligands with C–O values of 1.33 (1) Å. Unusually short Mo–O distances of 1.853 (7) and 1.869 (6) Å for the bridging ligands are consistent with strong donor character and significantly oxidized metal centers. These values are on the order of Mo–O distances observed for bridging oxo ligands (Mo–O–Mo) in Mo(V) and Mo(VI) structures.[23] In $Mo(PQ)_3$ we find a third mode of coordination for *o*-quinone ligands and a much less strongly oxidized metal. Two of the 9,10-phenanthrenequinone (PQ) ligands chelate normally to the metal with an average Mo–O distance of 1.952 (5) Å in close agreement with an average value of 1.949 (6) Å for the chelated ligands in $[Mo(O_2C_6Cl_4)_3]_2$. The carbon

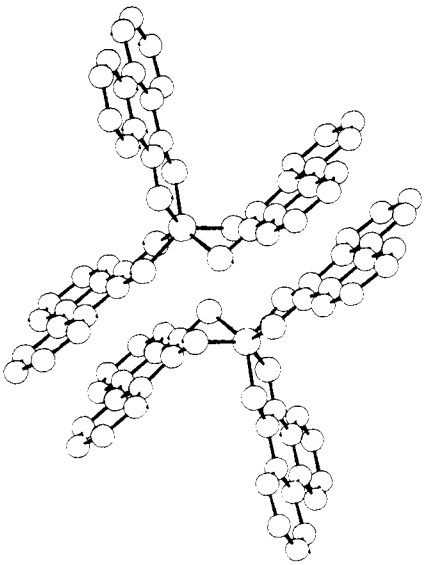

Figure 3. View of the contents of the unit cell. Separations between planes of ligands of adjacent molecules are on the order of 3.2–3.3 Å.

atom plane of the third quinone in $Mo(PQ)_3$ forms a dihedral angle of 119.7 (6)° with its MoO_2 chelate plane. The metal atom is located 1.22 Å above this plane. Carbonyl C–O distances of 1.34 (1) Å and C–C values of 1.35 (1) Å for the planar chelating ligands are comparable to related distances of chelating ligands in $[Mo(O_2C_6Cl_4)_3]_2$. The bent ligand is less reduced with C–O distances of 1.31 (1) Å and a C(1)–C(2) separation of 1.43 (1) Å consistent with greater benzoquinone character.[24] Thus we find a range of ligand oxidation states for the quinones extending from the highly reduced bridging ligands in $[Mo(O_2C_6Cl_4)_3]_2$ through the intermediate chelated ligands to the bent ligand in $Mo(PQ)_3$. It is of particular interest that the chelate plane of the quinone ligand is sufficiently flexible as to allow either planar or bent options, a feature not generally observed with unsaturated chelating ligands. The nature of the bond between the metal and the bent quinone is also unusual for an unsaturated oxygen donor ligand. The Mo–O–C bond angles of 92.6 (5)° suggest that the metal may interact directly with the out-of-plane p orbitals of the oxygens. Distances of 2.424 (8) Å to the carbonyl carbons may allow a significant bonding contribution from the carbonyl π-bond similar to the bonding in trigonal prismatic tris(methyl vinyl ketone)tungsten.[25]

The quinones also appear unique among related, unsaturated ligands in their ability to vary the ligand bite. The

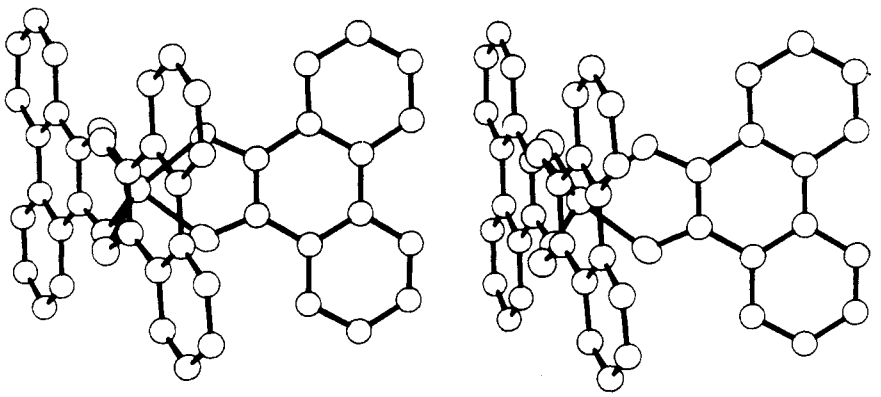

Figure 2. Stereoview of the entire $Mo(PQ)_3$ molecule showing the parallel orientation of the bent and chelating quinone ligands.

Table IV. Principal Intramolecular Bonding Parameters for $Mo(O_2C_{14}H_8)_3$

Bent Ligand			
Distances (Å)			
Mo–O(1)	1.969 (5)	C(6)–C(7)	1.415 (11)
Mo–O(2)	1.988 (5)	C(7)–C(8)	1.374 (11)
O(1)–C(1)	1.311 (8)	C(8)–C(9)	1.441 (12)
O(2)–C(2)	1.314 (8)	C(9)–C(10)	1.387 (12)
C(1)–C(2)	1.427 (10)	C(5)–C(10)	1.411 (11)
C(2)–C(3)	1.452 (10)	C(3)–C(11)	1.434 (11)
C(3)–C(4)	1.424 (10)	C(11)–C(12)	1.416 (11)
C(4)–C(5)	1.437 (11)	C(12)–C(13)	1.363 (12)
C(5)–C(6)	1.419 (10)	C(13)–C(14)	1.372 (12)
C(6)–C(1)	1.444 (10)	C(4)–C(14)	1.439 (11)
		Mo···C(1)	2.421 (8)
		Mo···C(2)	2.426 (8)
Angles (deg)			
Mo–O(1)–C(1)	92.9 (5)	O(1)–C(1)–C(6)	124.5 (8)
Mo–O(2)–C(2)	92.3 (5)	O(2)–C(2)–C(1)	116.9 (8)
O(1)–C(1)–C(2)	115.4 (7)	O(2)–C(2)–C(3)	123.5 (8)
Chelated Ligand I[a]			
Distances (Å)			
Mo–O(3)	1.947 (5)	C(20)–C(21)	1.415 (10)
Mo–O(4)	1.939 (5)	C(21)–C(22)	1.387 (10)
O(3)–C(15)	1.349 (8)	C(22)–C(23)	1.408 (11)
O(4)–C(16)	1.342 (8)	C(23)–C(24)	1.367 (11)
C(15)–C(16)	1.347 (10)	C(19)–C(24)	1.426 (10)
C(16)–C(17)	1.423 (10)	C(17)–C(25)	1.420 (11)
C(17)–C(18)	1.417 (10)	C(25)–C(26)	1.383 (10)
C(18)–C(19)	1.445 (10)	C(26)–C(27)	1.406 (11)
C(19)–C(20)	1.423 (10)	C(27)–C(28)	1.375 (11)
C(15)–C(20)	1.440 (10)	C(18)–C(28)	1.424 (10)
Angles (deg)			
Mo–O(3)–C(15)	117.6 (5)	O(3)–C(15)–C(20)	124.1 (7)
Mo–O(4)–C(16)	117.7 (5)	O(4)–C(16)–C(15)	114.1 (7)
O(3)–C(15)–C(16)	113.1 (7)	O(4)–C(16)–C(17)	124.2 (8)
Chelated Ligand II			
Distances (Å)			
Mo–O(5)	1.953 (5)	C(34)–C(35)	1.420 (11)
Mo–O(6)	1.969 (5)	C(35)–C(36)	1.413 (11)
O(5)–C(29)	1.343 (9)	C(36)–C(37)	1.391 (12)
O(6)–C(30)	1.349 (9)	C(37)–C(38)	1.365 (12)
C(29)–C(30)	1.349 (10)	C(33)–C(38)	1.424 (11)
C(30)–C(31)	1.446 (10)	C(31)–C(39)	1.402 (12)
C(31)–C(32)	1.430 (10)	C(39)–C(40)	1.388 (11)
C(32)–C(33)	1.428 (11)	C(40)–C(41)	1.407 (11)
C(33)–C(34)	1.410 (10)	C(41)–C(42)	1.365 (11)
C(29)–C(34)	1.442 (10)	C(32)–C(42)	1.430 (11)
Angles (deg)			
Mo–O(5)–C(29)	118.9 (5)	O(5)–C(29)–C(34)	125.4 (8)
Mo–O(6)–C(30)	116.2 (5)	O(6)–C(30)–C(29)	114.9 (8)
O(5)–C(29)–C(30)	113.1 (8)	O(6)–C(30)–C(31)	122.3 (8)
Interdonor Contacts and Angles about Mo Atom			
Distances (Å)			
O(1)···O(2)	2.584 (7)	O(3)···O(4)	2.426 (7)
O(1)···O(3)	2.573 (7)	O(3)···O(5)	2.621 (7)
O(1)···O(5)	2.673 (7)	O(4)···O(6)	2.616 (7)
O(2)···O(4)	2.560 (7)	O(5)···O(6)	2.449 (7)
O(2)···O(6)	2.709 (7)		
Angles (deg)			
O(1)–Mo–O(2)	81.5 (2)	O(2)–Mo–O(4)	81.3 (2)
O(3)–Mo–O(4)	77.2 (2)	O(2)–Mo–O(6)	86.4 (2)
O(5)–Mo–O(6)	77.2 (2)	O(3)–Mo–O(5)	84.4 (2)
O(1)–Mo–O(3)	82.1 (2)	O(4)–Mo–O(6)	84.0 (2)
O(1)–Mo–O(5)	85.9 (2)		

[a] Ligand paired with bent ligand of centrosymmetrically related molecule.

Table V. Dihedral Angles and Least-Squares Planes for $Mo(O_2C_{14}H_8)_3$

Dihedral Angles		
Plane 1	Plane 2	Angle (deg)
Mo, O(1), O(2)	Mo, O(3), O(4)	116.5 (2)
Mo, O(1), O(2)	Mo, O(5), O(6)	125.2 (2)
Mo, O(3), O(4)	Mo, O(5), O(6)	118.3 (2)
Mo, O(1), O(2)	O(1), O(2), C(1)	119.0 (5)
Mo, O(1), O(2)	O(1), O(2), C(2)	119.7 (5)

Least-Squares Planes[a, b]

Bent Ligand

$-3.73x + 7.94y + 5.02z = -1.09$

Atom	Distance (Å)	Atom	Distance (Å)
Mo	1.22	Mo'[c]	3.40
O(1)	−0.08	O(3)'	3.24
O(2)	−0.03	O(4)'	3.28
C(1)	−0.015 (8)	C(15)'	3.24
C(2)	−0.005 (8)	C(16)'	3.26
C(3)	0.023 (8)	C(17)'	3.31
C(4)	−0.020 (8)	C(18)'	3.40
C(5)	−0.001 (8)	C(19)'	3.38
C(6)	0.019 (8)	C(20)'	3.29
C(7)	0.08	C(21)'	3.26
C(8)	0.07	C(22)'	3.35
C(9)	0.01	C(23)'	3.46
C(10)	−0.05	C(24)'	3.47
C(11)	0.03	C(25)'	3.33
C(12)	−0.03	C(26)'	3.44
C(13)	−0.07	C(27)'	3.53
C(14)	−0.03	C(28)'	3.47

Chelated Ligand I

$-4.01x + 7.47y + 5.99z = -2.03$

Atom	Distance (Å)	Atom	Distance (Å)
Mo	0.33	C(21)	−0.03
O(3)	0.09	C(22)	−0.02
O(4)	0.11	C(23)	0.01
C(15)	0.003 (8)	C(24)	0.01
C(16)	0.016 (8)	C(25)	0.00
C(17)	−0.013 (8)	C(26)	0.02
C(18)	−0.000 (8)	C(27)	0.04
C(19)	−0.006 (8)	C(28)	0.00
C(20)	−0.015 (8)		

Chelated Ligand II

$4.14x + 9.27y - 13.05z = -0.15$

Atom	Distance (Å)	Atom	Distance (Å)
Mo	0.19	C(35)	−0.03
O(5)	0.10	C(36)	0.06
O(6)	0.13	C(37)	0.08
C(29)	−0.002 (8)	C(38)	0.05
C(30)	0.006 (8)	C(39)	−0.03
C(31)	−0.003 (8)	C(40)	−0.06
C(32)	−0.007 (8)	C(41)	−0.05
C(33)	0.013 (8)	C(42)	−0.04
C(34)	−0.008 (8)		

Trigonal Face I

$10.18x - 3.01y - 0.64z = 2.09$

Atom	Distance (Å)	Atom	Distance (Å)
Mo	1.25	O(4)	0.00
O(1)	2.58	O(5)	2.45
O(2)	0.00	O(6)	0.00
O(3)	2.42		

Trigonal Face II

$10.28x - 2.32y - 1.12z = 0.46$

Atom	Distance (Å)	Atom	Distance (Å)
Mo	−1.24	O(4)	−2.43
O(1)	0.00	O(5)	0.00
O(2)	−2.58	O(6)	−2.44
O(3)	0.00		

[a] Least-squares planes calculated according to W. C. Hamilton, *Acta Crystallogr.*, 14, 185 (1961). Equations given in triclinic coordinates. [b] Atoms listed without errors not included in the calculation of the plane. [c] Prime symbol refers to atoms of the complex molecule related to those of Table I by the crystallographic center of inversion.

Table VI. Trigonal Prismatic Complexes of Bidentate Donor Ligands

	$M(O-O)_3$	$M(S-S)_3$				$M(Se-Se)_3$
	$Mo(O_2C_{14}H_8)_3$[a]	$Mo(S_2C_2H_2)_3$	$Mo(S_2C_6H_4)_3$	$Re(S_2C_2(Ph)_2)_3$	$V(S_2C_2(Ph)_2)_3$	$Mo(Se_2C_2(CF_3)_2)_3$
M–X	1.952 (5)	2.33 (1)	2.367 (2)	2.325 (4)	2.338 (4)	2.492 (2)
X···X(intra)	2.438 (7)	3.10	3.110 (2)	3.032 (10)	3.060 (6)	3.317 (5)
X···X(inter)	2.619 (7)	3.11	3.091 (3)	3.050 (8)	3.065	3.222 (3)
X–M–X	77.2 (2)	82.5	*b*	81.4 (4)	81.7 (2)	83.4 (1)
M–X–C	117.5 (5)	*b*	*b*	109 (1)	109.6 (3)	105.1 (4)
X–C–C[c]	113.8 (5)	*b*	*b*	120 (2)	119.3 (7)	121.2 (4)
Ref		17	18	19	20	21

[a] Table includes only bonding parameters of planar, chelating quinone ligands. [b] Values not reported. [c] Angle on interior of chelate ring.

largest intraligand oxygen-oxygen separation occurs for the bridging ligands of $[Mo(O_2C_6Cl_4)_3]_2$ where a distance of 2.756 (8) Å is observed and O-C-C angles show no significant variation from 120°. With chelated ligands in both $Mo(PQ)_3$ and $[Mo(O_2C_6Cl_4)_3]_2$ the O-O contact decreases to about 2.42-2.43 Å with O-C-C angles interior to the chelate ring of 113°. Intermediate separations of 2.684 (8) and 2.584 (7) Å have been found for $Pd(PPh_3)_2(O_2C_6Cl_4)$[26] and the bent ligand in $Mo(PQ)_3$, respectively. This variation over approximately 0.33 Å is quite significant and, while the separation is coupled to the C-O bond length, the contraction of interior angles of the chelate ring in the Mo complexes points to a bonding interaction between donor atoms.

Trigonal Prismatic Coordination. Prior to the structural characterization of the neutral tris(1,2-dithiolene) complexes the trigonal prismatic geometry was confined mainly to solid state materials possessing the molybdenite structure. Recent work has yielded numerous examples with the geometry either imposed on metals with amorphous stereochemical preferences by rigid clathrochelate ligands[27] or arising from poorly understood electronic factors within the molecule. It is the latter class of compounds which are of particular interest. The unrestrained prismatic systems are observed primarily with metals on the left of the transition series, groups 5, 6, and 7, with bidentate ligands chelating along the edges of the prism. The widest variety of prismatic molecules have been observed with the metals Mo and W. These include the organometallic complexes tris(butadiene)molybdenum[28] and tris(methyl vinyl ketone)tungsten[25] and the neutral tris(1,2-dithiolene) and diselenolene complexes. Long carbonyl and olefin bond lengths in $W(H_2CCHCO(CH_3))_3$[25] and short carbon-sulfur distances in the dithiolene structures suggest oxidation states for the metals intermediate between the formal charges of zero and +6 for the two types of complexes. Studies on the tris(1,2-dithiolene) systems with ligands of varying electron withdrawing ability have shown that the neutral prismatic complexes are least stable with the most strongly oxidizing ligands.[4] The observed octahedral geometries of the tris(tetrachloro-1,2-benzoquinone) complexes of Cr, Mo, and W with the prismatic geometry of $Mo(PQ)_3$ suggest that within an isoelectronic series stereochemistry may also be determined by the acceptor nature of the ligand.

Dimensions of the MoX_6 prismatic units with variation of the donor atom from oxygen to selenium follow consistent trends (Table VI). The most regular structure is observed with the sulfur donor ligands where inter- and intradonor separations are essentially equivalent and the tetragonal faces of the prism are square. For the $MoSe_6$ prism distances along trigonal faces are shorter than intraligand distances along edges while the opposite is true of the MoO_6 prism. It is of interest that had the intraligand O-O separation been closer to the value of 2.684 (8) Å observed in $Pd(PPh_3)_2(O_2C_6Cl_4)$ the MoO_6 prism would be far more regular. As might be expected bite angles of the ligands are smallest for the oxygen donors (77.2 (2)°) and largest for the Se system (83.4 (1)°). The larger M-X-C and smaller X-C-C angles for the oxygen donor complex are consistent with a distortion within the chelate ring requiring the oxygen donors to be proportionately closer together than the S and Se donors.

Intermolecular Charge-Transfer Bonding. Quinones are well known for their ability to form charge-transfer complexes with other planar unsaturated organic molecules.[29,30] This affinity seems also to be a property of quinone ligands. Samples of the tetrachloro-1,2-benzoquinone complexes of Cr, Mo, and W isolated from benzene are found to be extensively solvated. The structure determination on $[Mo(O_2C_6Cl_4)_3]_2 \cdot 3C_6H_6$ has shown benzene molecules sandwiched interstitially between planes of chelating ligands of adjacent molecules. Each complex molecule is linked to four neighbors by benzene bridges resulting in a two-dimensional polymeric array. Interplanar separations range from 3.4 to 3.5 Å, normal for such stacked aromatic systems. Samples of $Mo(PQ)_3$ isolated from benzene are found to be unsolvated. Rather, adjacent complex molecules related by the crystallographic center of inversion pair together forming a strong charge-transfer couple. Separations between ligand atoms and least-squares plane of the adjacent ligand are as close as 3.24 Å (Table V). This value is comparable to separations in benzoquinone-hydroquinone donor-acceptor complexes where values of 3.2 Å are commonly observed[30] and separations in the conductive 2,2′-bis-1,3-dithiole (TTF)-7,7,8,8-tetracyanoquinodimethane (TCNQ) system where values of 3.17 and 3.47 Å are observed for the TCNQ and TTF stacks, respectively.[31]

Acknowledgment. We wish to thank Mr. Hartley Downs for his help with data collection and also the Research Corporation and West Virginia University for their support of this research.

Supplementary Material Available. A listing of structure factor amplitudes will appear following these pages in the microfilm edition of this volume of the journal. Photocopies of the supplementary material from this paper only or microfiche (105 × 148 mm, 24× reduction, negatives) containing all of the supplementary material for the papers in this issue may be obtained from the Journals Department, American Chemical Society, 1155 16th St., N.W., Washington, D.C. 20036. Remit check or money order for $4.00 for photocopy or $2.50 for microfiche, referring to code number JACS-75-4912.

References and Notes

(1) Y. S. Sohn and A. L. Balch, *J. Am. Chem. Soc.*, **94**, 1144 (1972), and references therein.
(2) A. E. Martell and M. M. Taqui Kahn, "Inorganic Biochemistry", G. L. Eichhorn, Ed., Elsevier, Amsterdam, 1973..
(3) J. T. Spence and P. Kronek, *J. Less-Common Met.*, **36**, 465 (1974).
(4) (a) J. A. McCleverty, *Prog. Inorg. Chem.*, **10**, 49 (1968); (b) G. N. Schrauzer, *Acc. Chem. Res.*, **2**, 72 (1969); (c) R. Eisenberg, *Prog. Inorg. Chem.*, **12**, 925 (1970).
(5) F. Rohrscheid, A. L. Balch, and R. H. Holm, *Inorg. Chem.*, **5**, 1542 (1966).

(6) C. Floriani, R. Henzi, and F. Calderazzo, *J. Chem. Soc., Dalton Trans.*, 2640 (1972).
(7) S. Prasad and K. S. R. Krishnaiah, *J. Indian Chem. Soc.*, **37**, 681 (1960).
(8) C. G. Pierpont, H. H. Downs, and T. G. Rukavina, *J. Am. Chem. Soc.*, **96**, 5573 (1974).
(9) C. G. Pierpont and H. H. Downs, *J. Am. Chem. Soc.*, **97**, 2123 (1975).
(10) C. G. Pierpont and R. M. Buchanan, *J. Am. Chem. Soc.*, in press.
(11) T. C. Furnas, "Single Crystal Orienter Instruction Manual", General Electric Co., Milwaukee, Wis., 1957, Chapter 10.
(12) J. Reed, A. J. Schultz, C. G. Pierpont, and R. Eisenberg, *Inorg. Chem.*, **12**, 2949 (1973).
(13) D. T. Cromer and J. T. Waber, *Acta Crystallogr.*, **18**, 104 (1965).
(14) R. F. Stewart, E. R. Davidson, and W. T. Simpson, *J. Chem. Phys.*, **42**, 3175 (1965).
(15) D. T. Cromer and D. Liberman, *J. Chem. Phys.*, **53**, 1891 (1970).
(16) See paragraph at end of paper regarding supplementary material.
(17) A. E. Smith, G. N. Schrauzer, V. P. Mayweg, and W. Heinrich, *J. Am. Chem. Soc.*, **87**, 5798 (1965).
(18) M. J. Bennett, M. Cowie, J. L. Martin, and J. Takats, *J. Am. Chem. Soc.*, **95**, 7504 (1973).
(19) R. Eisenberg and J. A. Ibers, *Inorg. Chem.*, **5**, 411 (1966).
(20) R. Eisenberg and H. B. Gray, *Inorg. Chem.*, **6**, 1844 (1967).
(21) C. G. Pierpont and R. Eisenberg, *J. Chem. Soc. A*, 2285 (1971).
(22) (a) M. C. Glick and L. F. Dahl, *J. Organomet. Chem.*, **3**, 200 (1965); (b) G. G. Aleksandrov, Yu. T. Struchkov, V. S. Khandkarova, and S. P. Gubin, *ibid.*, **25**, 243 (1970).
(23) See, for example, F. A. Cotton, *J. Less-Common Met.*, **36**, 13 (1974).
(24) For a review of the structural properties of quinones see J. Bernstein, M. D. Cohen, and L. Leiserowitz, "The Chemistry of the Quinonoid Compounds", S. Patai, Ed., Interscience, New York, N.Y., 1974.
(25) R. E. Moriarty, R. D. Ernst, and R. Bau, *J. Chem. Soc., Chem. Commun.*, 1242 (1972).
(26) C. G. Pierpont and H. H. Downs, *Inorg. Chem.*, **14**, 343 (1975).
(27) (a) W. O. Gillum, R. A. D. Wentworth, and R. F. Childers, *Inorg. Chem.*, **9**, 1825 (1970); (b) M. R. Churchill and A. H. Reis, *ibid.*, 11, 1811 (1972).
(28) M. M. Yevitz and P. S. Skell, Abstract E9, American Crystallographic Association Meeting, University Park, Pa., Aug 1974.
(29) R. Foster, "Organic Charge-Transfer Complexes", Academic Press, London, 1969.
(30) R. Foster and M. I. Foreman, ref 24.
(31) T. J. Kistenmacher, T. E. Phillips, and D. O. Cowan, *Acta Crystallogr., Sect. B*, **30**, 763 (1974).

Hyperfine Coupling Patterns in the 2,3-Naphthobarrelene and 2,3-Naphthobarrelane Radical Anions

John R. Dodd* and George V. Sanzero

Contribution from the Department of Chemistry, Emory University, Atlanta, Georgia 30322.
Received February 4, 1975

Abstract: The radical anions of 2,3-naphthobarrelene (**2**) and 2,3-naphthobarrelane (**3**) were studied by ESR spectroscopy and polarography in order to investigate the importance of long-range coupling, 1,3-π-π interaction, ion pairing phenomena, and steric and strain effects in these species. The magnitudes of the two largest hyperfine splitting constants (hfsc's) of $\mathbf{2}\cdot^-$ and $\mathbf{3}\cdot^-$ were found to vary appreciably as a function of the solvent and the counterion; these variations are interpreted in terms of ion pairing phenomena. The relative importance of the combined effects of electron repulsion and steric desolvation by the bicyclic moieties versus the effect of strain due to the bicyclic moieties is believed to determine which aromatic protons have the largest hfsc in these species. Analysis of the observed variations in the hfsc's in conjunction with a model for the lowest energy ion pair of $\mathbf{2}\cdot^-$ or $\mathbf{3}\cdot^-$ was used to assign the two largest hfsc's in both radical anions and to consequently indicate the relative importance of the above effects.

Studies of the hyperfine coupling patterns of complex radical anions as a function of their structure and geometry are a topic of continuing interest.[1] The extent and mechanisms of long-range hyperfine coupling (i.e., coupling at or beyond the γ position relative to the radical center(s), see structure **1**) in radical species in recent years, for example, has received much attention in the literature.[2] Long-range hyperfine couplings (hfsc's) of varying magnitudes have been observed in many rigid polycyclic radical anions, including those containing the semidione,[2a] semiquinone,[2b,c] and semifuraquinone[2d] spin labels.

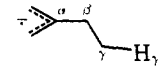

1

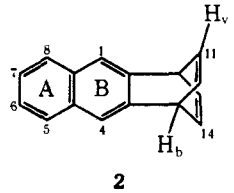

2

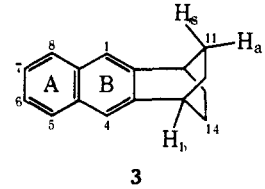

3

Few studies[3] of aromatic radical anions containing a fused bicyclic (or higher polycyclic) ring,[4] however, have been reported. In the present paper, we wish to report the results of a study of the hyperfine coupling patterns in the radical anions of 2,3-naphthobarrelene (**2**, 1,4-etheno-1,4-dihydroanthracene) and 2,3-naphthobarrelane (**3**, 1,4-ethano-1,2,3,4-tetrahydroanthracene).

Results

The radical anion of **2** was generated for ESR study by reduction of a dilute solution (1.0×10^{-3} *M*)[5] of **2** in various ethereal solvents at low temperatures with an alkali metal. Two of the hfsc's of $\mathbf{2}\cdot^-$ were found to vary significantly with the solvent and the counterion as illustrated by the data in Table I. The small pentet splitting of ~0.13 G was generally resolved only at lower temperatures. Line width alternation and metal coupling were not observed under any of the conditions studied. Simulations of the experimental ESR spectra (using a computer program which assumes a Lorentzian line shape) were performed using each of the sets of hfsc's shown in Table I. In each case, the simulated ESR spectrum was in excellent agreement with the experimental ESR spectrum.

Similarly the radical anion of **3** was generated for ESR study by reduction of a dilute solution (2.0×10^{-3} *M*)[6] of **3** in various ethereal solvents with an alkali metal. Appreciable variations of two of the hfsc's of $\mathbf{3}\cdot^-$ were also observed upon change of the solvent and counterion, as the data in Table II indicate. Line width alternation and metal coupling were not observed for this radical anion under any of the conditions studied. Each of the experimental ESR spectra corresponding to the sets of hfsc's shown in Table II was